

# New HST Observations of High Velocity Ly $\alpha$ and H $\alpha$ in SNR 1987A

Eli Michael<sup>1</sup>, Richard McCray<sup>1</sup>, C. S. J. Pun<sup>2</sup>, Kazimierz Borkowski<sup>3</sup>, Peter Garnavich<sup>4</sup>, Peter Challis<sup>4</sup>, Robert P. Kirshner<sup>4</sup>, Roger Chevalier<sup>5</sup>, Alexei Fillippenko<sup>6</sup>, Claes Fransson<sup>7</sup>, Nino Panagia<sup>8</sup>, Mark Phillips<sup>9</sup>, Brian Schmidt<sup>10</sup>, Nicholas Suntzeff<sup>9</sup>, and J. Craig Wheeler<sup>11</sup>

## ABSTRACT

We describe and model high velocity ( $\approx 15,000 \text{ km s}^{-1}$ ) Ly $\alpha$  and H $\alpha$  emission from supernova remnant 1987A seen in September and October 1997 with the Space Telescope Imaging Spectrograph. Part of this emission comes from a reverse shock located at  $\approx 75\%$  of the radius of the inner boundary of the inner circumstellar ring and confined within  $\pm 30^\circ$  of the equatorial plane. Departure from axisymmetry in the Ly $\alpha$  and H $\alpha$  emission correlates with that seen in nonthermal radio emission and reveals an asymmetry in the circumstellar gas distribution. We also see diffuse high velocity Ly $\alpha$  emission from supernova debris inside the reverse shock that may be due to excitation by nonthermal particles accelerated by the shock.

*Subject headings:* supernova remnants: individual (SNR 1987A) – circumstellar matter – shocks

---

<sup>1</sup>JILA, University of Colorado, Boulder, CO 80309-0440; michael@colorado.edu; dick@jila.colorado.edu

<sup>2</sup>Laboratory for Astronomy and Space Physics, Code 681, NASA - GSFC, Greenbelt, MD 20771; pun@congee.gsfc.nasa.gov

<sup>3</sup>Dept. of Physics, North Carolina State University, Raleigh, NC 27695; kazik@mozart.physics.ncsu.edu

<sup>4</sup>Harvard-Smithsonian Center for Astrophysics, 60 Garden St, Cambridge, MA 02138; (pgarnavich,pchallis,kirshner)@cfa.harvard.edu

<sup>5</sup>Dept. of Astronomy, University of Virginia, P.O. Box 3818, Charlottesville, VA 22903-0818

<sup>6</sup>Dept. of Astronomy, University of California, Berkeley, CA 94720

<sup>7</sup>Stockholm Observatory, S-133 36 Saltsjöbaden, Sweden

<sup>8</sup>STScI, 3700 San Martin Drive, Baltimore, MD 21218

<sup>9</sup>CTIO, NOAO, Casilla 603, La Serena, Chile

<sup>10</sup>Mount Stromlo and Siding Spring Observatory, Private Bag, Weston Creek P.O., Australia

<sup>11</sup>Dept. of Astronomy and McDonald Observatory, University of Texas, Austin, TX 78712

## 1. Introduction

On May 24, 1997 (day 3743 after core collapse), Sonneborn *et al.* (1998) observed supernova remnant (SNR) 1987A with the Space Telescope Imaging Spectrograph (STIS). They discovered very broad ( $\approx 20,000 \text{ km s}^{-1}$ ) Ly $\alpha$  emission in the ultraviolet spectrum. Michael *et al.* (1998, hereafter M98) interpreted this emission as the result of excitation of neutral hydrogen atoms in the supernova debris crossing a reverse shock. The observed Ly $\alpha$  flux was close to the value predicted by Borkowski *et al.* (1997, hereafter B97) for such a model normalized to account for the soft X-ray flux observed by ROSAT. M98 also pointed out that the broad Ly $\alpha$  emission should be accompanied by H $\alpha$  emission that should be observable both from the ground and with STIS.

The observations reported by Sonneborn *et al.* (1998) were taken with a  $2'' \times 2''$  aperture that included the entire inner circumstellar ring of SNR 1987A. With  $24 \text{ \AA arcsec}^{-1}$  dispersion, the resulting Ly $\alpha$  image seen on the STIS detector is a convolution of the spatial ( $\approx 1''$ ) and velocity ( $\approx 3''$ ) structure of the emitting region. M98 found that they could fit the observed image with a model in which the shock surface was a prolate ellipsoid slightly elongated in the direction normal to the ring plane, but they found evidence for an additional source of diffuse emission inside the shock surface. This result was surprising, because the model in B97, following Chevalier & Dwarkadas (1995), implies that most of the emission should come from a ring shaped surface inside the inner circumstellar ring.

Here we report a new set of STIS observations of the fast shocks in SNR 1987A, this time taken with slits covering only part of the emitting region and including H $\alpha$  as well as Ly $\alpha$ . These new observations enable us to distinguish the dynamics and morphology of the fast shocks more clearly. We now see that the shock emission is indeed concentrated in the equatorial plane, contrary to our interpretation of the earlier STIS observations. We also see a diffuse component of emission that may indicate excitation and ionization by nonthermal particles. We have not yet detected an unambiguous signal from high velocity N V  $\lambda\lambda 1239, 1243$  emission.

The same set of observations also provides new information on the spectra of the supernova ejecta and the circumstellar ring, including a rapidly brightening “hot spot” that is apparently caused by the first encounter of the supernova blast wave with the ring. We will interpret those data in subsequent papers.

## 2. Observations

The Supernova Intensive Study (SINS) collaboration obtained STIS spectra of SNR 1987A in ultraviolet and optical wavelengths in September and October 1997 respectively. The ultraviolet spectrum, which covers the wavelength range 1130 – 1720 Å, was taken on JD 2,450,719.1, or 3869.3 days since explosion, with the G140L low dispersion grating ( $\Delta v \approx 300 \text{ km s}^{-1}$  at Ly $\alpha$ ). The resolution along the spatial direction is  $\approx 0''.06$ . Five spectral images totaling 11200 sec of exposure were combined. The optical spectrum, which covers the wavelength range 5260 – 10260 Å, was taken on JD 2,450,727.8, or 3878.0 days since explosion, with the G750L low resolution grating ( $\Delta v \approx 450 \text{ km s}^{-1}$  at H $\alpha$ ). The spatial resolution is  $\approx 0''.1$ . Two spectral images totaling 4800 sec of exposure were obtained. The two images were dithered along the orientation of the slit so that both cosmic ray hits and hot pixels on the STIS/CCD were removed simultaneously in the final combined data.

Figure 1a illustrates the slit positions on the inner circumstellar ring for the two observations. A  $0''.5$  slit was used for Ly $\alpha$  and a  $0''.2$  slit was used for H $\alpha$ . Both slits were offset  $0''.1$  to the SE of the centroid of the ring, with position angles of  $-147^\circ$  and  $-139^\circ$  for the Ly $\alpha$  and H $\alpha$  observations, respectively.

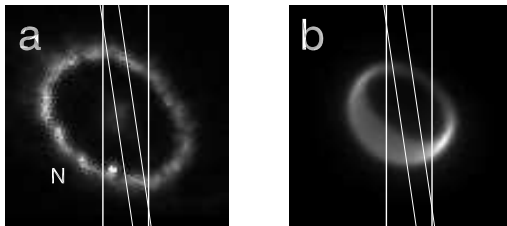


Fig. 1.— (a) The position of the Ly $\alpha$  (wide) and H $\alpha$  (narrow) slits on the inner ring, **N** denotes the northern side of the remnant. (b) position of the slits on the reverse shock surface which lies at  $\approx 70\%$  of the distance to the inner ring.

Figure 2a shows the ultraviolet spectrum in the vicinity of Ly $\alpha$ . It displays the following components: (1) bright stationary geocoronal Ly $\alpha$  emission filling the slit; (2) a nearly horizontal streak of intense blue-shifted Ly $\alpha$  emission below the centerline but inside the lower (NE) side of the ring extending to  $-15,000 \text{ km s}^{-1}$ ; (3) a fainter horizontal streak of red-shifted emission above the centerline but inside the upper (SW) side of the ring extending to  $12,000 \text{ km s}^{-1}$ ; (4) a vertical band at  $4000 - 8000 \text{ km s}^{-1}$  due to diffuse, N v  $\lambda\lambda 1239, 1243$  emission from nearly stationary N v ions in the vicinity of the ring; and (5) a broad component of diffuse emission extending from  $-15,000$  to  $20,000 \text{ km s}^{-1}$ .

Figure 2c shows the optical spectrum in the vicinity of H $\alpha$ . It displays the following

components: (1) pairs of bright spots above and below the centerline due to emission by the nearly stationary inner ring at [O I]  $\lambda\lambda 6300, 6364$ , [N II]  $\lambda\lambda 6548, 6584$ ,  $H\alpha$ , and [S II]  $\lambda\lambda 6717, 6731$ ; (2) broad horizontal bands along the centerline due to emission in these same lines from atoms in the inner supernova debris excited by radioactivity; and (3) a nearly horizontal streak of blue-shifted  $H\alpha$  emission below the centerline but inside the circumstellar ring extending to  $-12,000 \text{ km s}^{-1}$ .

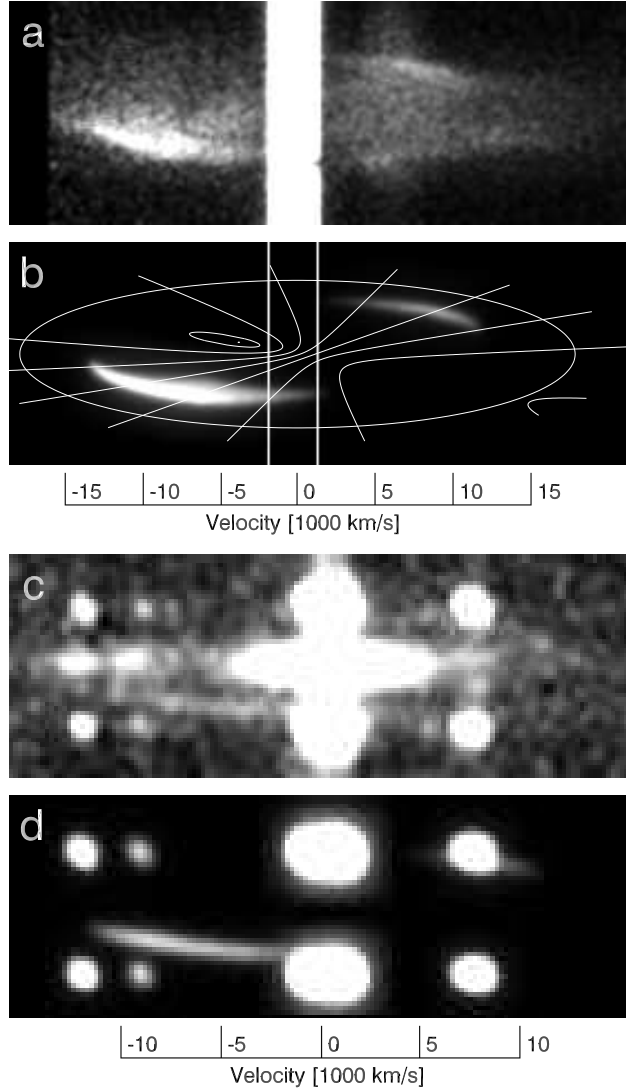


Fig. 2.— (a) STIS G140L spectrum of SNR 1987A in the vicinity of  $\text{Ly}\alpha$ . (b) Simulated STIS image of  $\text{Ly}\alpha$  emission from the reverse shock surface. (c) STIS G750L spectrum of SNR 1987A centered on  $\text{H}\alpha$ . (d) Simulated STIS image of line emission from the stationary ring and  $\text{H}\alpha$  emission from the reverse shock surface. The velocity scales are line of sight velocity measured from LMC rest frame.

### 3. Reverse Shock Emission

According to B97 and M98, we expect to see Ly $\alpha$  and H $\alpha$  emission from H I atoms in the supernova ejecta that are excited by electron and ion impacts as they cross a reverse shock. (We do not expect to see Ly $\alpha$  and H $\alpha$  emission from the blast wave because it is entering a region where the hydrogen atoms are already nearly fully ionized.) Since the H I atoms are freely streaming, with radial velocity  $\mathbf{v} = \mathbf{r}/t$ , before they cross the shock surface, the Doppler shifts of the Ly $\alpha$  and H $\alpha$  are determined by the geometry of the surface. M98 inferred from the earlier STIS observations that the reverse shock surface was a slightly prolate ellipsoid. For such a model, they predicted that a STIS observation of Ly $\alpha$  through a 0.5 slit would appear as an elliptical image (their Fig. 1d).

The actual STIS images of Ly $\alpha$  and H $\alpha$  (Figs. 2a,c) do not agree well with the prolate ellipsoid model for the reverse shock. Instead, they agree better with the model proposed by B97, in which the reverse shock emission is confined primarily to an equatorial band. We find also that the position and shape of the reverse shock surface vary from the far to the near side of the remnant, and probably on smaller scales as well.

We can fit both the blue-shifted Ly $\alpha$  and H $\alpha$  observations with a model in which the shock on the near side has a radius which ranges from  $0.73R_{ring}$  on the left side of the 0.5 slit to  $0.70R_{ring}$  on the right side of the slit and extends in latitude from  $30^\circ$  to  $-20^\circ$ .

To fit the red-shifted Ly $\alpha$  observations, the shock surface on the far side must have a radius  $0.76R_{ring}$  and extend in latitude from  $10^\circ$  to  $-5^\circ$ . The red-shifted H $\alpha$  emission was too faint to measure.

Figure 1b illustrates the reverse shock surface and its orientation in the slits for the Ly $\alpha$  and H $\alpha$  observations. The surface outside of the slits is not constrained by the present data and is shown only as an extrapolation. Figures 2b,d show the resulting model Ly $\alpha$  and H $\alpha$  STIS images, respectively. Lines of constant latitude are shown on the simulated Ly $\alpha$  image assuming that all the emission comes from the center of the slit (see §4). Comparison of the model Ly $\alpha$  and H $\alpha$  images demonstrates the advantage of a narrow slit in mapping the shock surface.

When we subtract the simulated images from the actual observations, the streaks vanish, leaving residual emission in the Ly $\alpha$  observation, which we discuss below in §4. The measured flux from the Ly $\alpha$  shock emission is  $(8.6 \pm 2.6) \times 10^{-15}$  ergs cm $^{-2}$  s $^{-1}$  on the blue side and  $(1.8 \pm 0.8) \times 10^{-15}$  ergs cm $^{-2}$  s $^{-1}$  on the red side. The measured flux from the H $\alpha$  shock emission is  $(6.0 \pm 1.8) \times 10^{-16}$  ergs cm $^{-2}$  s $^{-1}$  on the blue side and  $< 4 \times 10^{-16}$  ergs cm $^{-2}$  s $^{-1}$  on the red side.

The blue-shifted Ly $\alpha$  flux from the shock is greater than the red-shifted flux by a factor of  $\approx 4.8$ . If we assume that the outer SN debris is spherically symmetric with a power law density profile given by  $\rho(r, t) \propto t^{-3}(r/t)^{-9}$  (Eastman & Kirshner 1989), we can attribute this asymmetry to: the difference in shock radius (which contributes a factor  $\approx 1.7$ ); the fact that the reverse shock has a greater surface area on the near side (a factor  $\approx 2.1$ ), and the  $\approx 0.3$  year difference in light-travel time from the near side of the shock surface to the far side (a factor  $\approx 1.3$ ).

This asymmetry should not come as a great surprise. Gaensler *et al.* (1997) found that the nonthermal radio emission seen inside the inner circumstellar ring was much brighter on the northeast side than on the southwest side. The asymmetry in the reverse shock surface is not caused by an asymmetry in the supernova debris because then the red-shifted Ly $\alpha$  emission would be brighter due to the higher mass flux (ram pressure) required to drive the shock to a greater radius. The asymmetry therefore represents an asymmetry in the circumstellar gas distribution which the ejecta is encountering (the circumstellar gas on the far side must be more tenuous than the near side).

M98 calculated that, for the conditions behind the reverse shock, approximately 1 Ly $\alpha$  and 0.2 H $\alpha$  photons will be emitted per H I atom entering the shock. We can infer this emissivity ratio from the observations and our model, which allows us to correct for the fact that the Ly $\alpha$  observation is taken through a wider slit than the H $\alpha$  observation. Correcting for interstellar extinction factors of 0.15 at Ly $\alpha$  and 0.63 at H $\alpha$  (Fitzpatrick *et al.* 1990) we find, on the blue-shifted side, where the H $\alpha$  streak is bright enough to measure, this ratio to be  $4.6 \pm 2$ , consistent with our expectation.

Since we know the number of Ly $\alpha$  photons emitted per H I atom crossing the shock surface, we can infer the normalization [ $A$ , the density at  $(r/t) = 10,000 \text{ km s}^{-1}$  and  $t = 10$  years] of the SN envelope’s density profile from our model for the shock surface. Estimating that the reverse shock is propagating outward with velocity  $V_{rs} = 4,000 \text{ km s}^{-1}$  (B97) and assuming a helium number density  $n_{\text{He}} = 0.2n_{\text{H}}$ , we find  $A = 170 \pm 60 \text{ amu cm}^{-3}$ , which may be compared with Shigeyama & Nomoto’s (1990) model 14E1 ( $A = 120 \text{ amu cm}^{-3}$ ) and Woosley’s (1988) model 10H ( $A = 360 \text{ amu cm}^{-3}$ ). If we had taken the value of  $V_{rs}$  inferred from radio observations of the remnant (Gaensler *et al.* 1997),  $A$  would be decreased by  $\approx 10\%$ .

#### 4. Diffuse Emission

When we subtract the model images from the actual images, a diffuse component of high velocity  $\text{Ly}\alpha$  emission remains. This component was evident in the earlier slitless observation by Sonneborn *et al.* (1998), and led M98 to interpret those data with a model in which the reverse shock surface had the shape of a slightly prolate ellipsoid. Now, with the present observations, we can see clearly that the  $\text{Ly}\alpha$  and  $\text{H}\alpha$  emission from the reverse shock is confined to the equatorial plane, and that the residual  $\text{Ly}\alpha$  emission comes from a volume interior to that surface. A corresponding diffuse component of  $\text{H}\alpha$  presumably exists, but it is too faint to be seen with the present exposure.

To analyze the distribution of the diffuse  $\text{Ly}\alpha$  emission, we assume that the emitting gas is everywhere in free expansion. If so, and if the slit were very narrow, there would be a unique mapping from the STIS image to depth within the supernova debris. From such a mapping, we could reconstruct a two-dimensional image of the supernova debris intercepted by the slit. Figures 3a-c are just such images, where the coordinates are radius and latitude measured from the equatorial plane of the inner circumstellar ring. The curves of constant latitude are not radial lines because the slit is off-center.

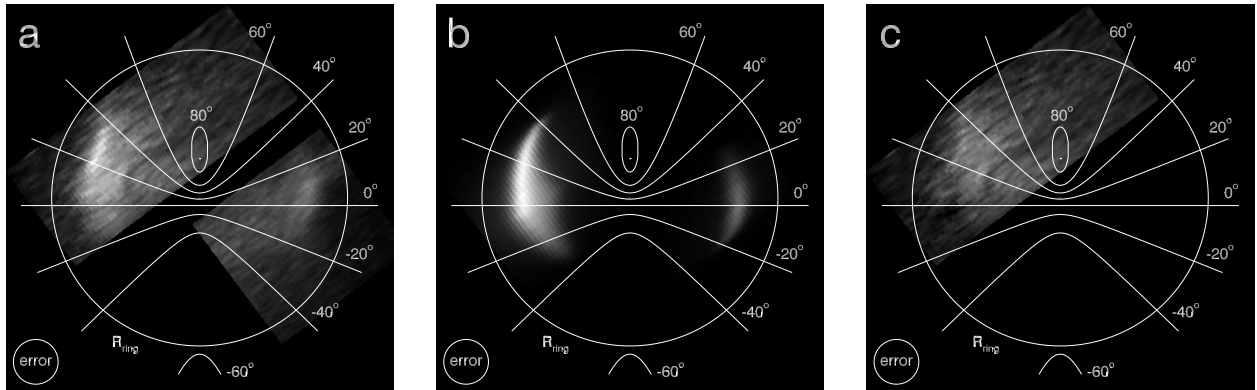


Fig. 3.— Remapping of  $\text{Ly}\alpha$  emission where appropriate, see text (§4). (a) observed emission, (b) simulated reverse shock emission, and (c) interior blue-shifted emission (panel (b) subtracted from panel (a)).

Figure 3a represents the  $\text{Ly}\alpha$  data of Figure 2a in such a coordinate system, in which we assume that the slit is a line centered in the actual slit. Since the actual slit has width  $0''.5$ , the mapping is not unique; this introduces a “point-spread function” for the mapping represented approximately by the error circles in Figures 3a-c.

Since we cannot distinguish the contribution of red-shifted  $\text{Ly}\alpha$  from that of  $\text{N v } \lambda\lambda 1239, 1243$  with the present data, we cannot interpret the signal on the lower right hand

side of Figure 3a.

Figure 3b represents the model for Ly $\alpha$  emission from the reverse shock surface corresponding to Figure 1b, including the broadening due to the 0".5 slit. In this coordinate system, we can see clearly that the blue-shifted Ly $\alpha$  emission comes from a reverse shock surface that lies primarily above the equatorial plane.

Figure 3c shows the residual flux on the blue side of Ly $\alpha$  after subtracting the contribution from the reverse shock from the data. This diffuse Ly $\alpha$  emission comes from supernova debris inside the reverse shock surface and appears to have a roughly uniform radial distribution. Like the Ly $\alpha$  emission from the reverse shock surface, the diffuse Ly $\alpha$  emission is strongest within latitudes 0° to 40°; but we see significant diffuse emission from –20° to 90°.

The flux of diffuse blue-shifted Ly $\alpha$  seen through the 0".5 slit is  $(5.7 \pm .3) \times 10^{-14}$  ergs cm $^{-2}$  s $^{-1}$ , or  $\approx 7$  times the flux of blue-shifted Ly $\alpha$  from the reverse shock. Each pixel in the spectrum observes a volume element in the debris so we are able to measure the volume emissivity of the diffuse interior emission. Correcting for interstellar extinction and assuming a distance of 50 kpc to the remnant we find this emissivity to be  $\approx 4 \times 10^{-19}$  ergs cm $^{-3}$  s $^{-1}$ .

What causes this diffuse emission? Since it is concentrated in the same latitude range as the reverse shock emission, one is tempted to look at the reverse shock itself as the source of the excitation. We can rule out one obvious candidate — soft X-rays emitted by the shock — because the soft X-ray luminosity observed by ROSAT (Hasinger et al. 1996) is roughly an order of magnitude too faint to account for the diffuse Ly $\alpha$ . Likewise, the hot spot is still too faint to cause significant diffuse Ly $\alpha$  emission. We suspect that the diffuse Ly $\alpha$  emission is caused by nonthermal particles that are accelerated at the reverse shock and diffuse into the freely expanding supernova envelope. We know that such particles are present from observations of nonthermal radio emission (Gaensler *et al.* 1997). The reverse shock may be a fairly efficient source of nonthermal particles (Jones & Ellison 1991). Moreover, those nonthermal particles that diffuse into the supernova envelope and deposit their energy may produce Ly $\alpha$  photons with efficiency approaching  $\approx 30\%$ .

## 5. Future Investigations

Further observations with STIS will give us a much clearer picture of the complex dynamics and kinetics of this extraordinary event. It would be valuable to observe the system again in the same slit configurations to measure the rate of brightening in Ly $\alpha$  and



H $\alpha$  emission from the shock surface. We should map the high velocity emission from the entire system, especially near the east side where the radio lobes are brightest.

As M98 have emphasized, observations of the line profile of high velocity N v  $\lambda\lambda 1239, 1243$  emission will provide a unique probe of the kinetics of a collisionless shock. We believe that the emission seen on the red side of Ly $\alpha$  contains a significant contribution from N v  $\lambda\lambda 1239, 1243$ , but we cannot distinguish this emission from Ly $\alpha$  emission in the present observations. To do that, we must observe the high velocity emission from the same part of SNR 1987A with STIS in both Ly $\alpha$  and H $\alpha$ . The exposure should be deep enough to see the diffuse emission clearly in H $\alpha$  as well as Ly $\alpha$ , and the slit should be narrow in order to separate the spatial structure from the velocity structure and to isolate the N v  $\lambda\lambda 1239, 1243$  emission from stationary gas. Then, since the ratio of Ly $\alpha$ /H $\alpha$  should be constant, we would be able to subtract the H $\alpha$  image from the Ly $\alpha$  image, leaving a remainder that is due to N v  $\lambda\lambda 1239, 1243$ .

This research was supported by NASA through grant No. GO-2563.01-87A from the Space Telescope Science Institute, which is operated by the Association of Universities for Research in Astronomy, Inc., under NASA contract NAS 5-26555, and by NASA grants NAG 5-3313 to the University of Colorado and 5-2844 to North Carolina State University. C. S. J. P. acknowledges funding by the STIS IDT through the National Optical Astronomy Observatories, and by the Goddard Space Flight Center.

## REFERENCES

- Borkowski, K., Blondin, J., & McCray, R. 1997, ApJ, 476, L31 (B97)
- Chevalier, R. A., & Dwarkadas, V. V. 1995, ApJ, 452, L45
- Eastman, R. G., & Kirshner, R. P. 1989, ApJ, 347, 771
- Fitzpatrick, E. L., & Walborn, N. R. 1990, AJ, 99, 1483
- Gaensler, B. M., Manchester, R. N., Staveland-Smith, L., Tzioumis, A. K., Reynolds, J. E., & Kesteven, M. J. 1997, ApJ, 479, 845
- Hasinger, G., Aschenbach, B., & Trümper, J. 1996, A&A, 312, L9
- Jones, F. C., & Ellison, D. C., Space Sci. Rev., 58, 259
- Michael, E., McCray, R., Borkowski, K. J., Pun, C. S. J., Sonneborn, G. 1998, ApJ, 492, L143 (M98)

Shigeyama, T., & Nomoto, K. 1990 ,ApJ, 360, 242

Sonneborn, G., *et al.* 1998, ApJ, 492, L139

Woosley, S. E. 1988, ApJ, 330, 218